HUNGARIAN JOURNAL OF
INDUSTRY AND CHEMISTRY
HJIC

OPTIMISATION OF THE PHYSICAL PROPERTIES OF RICE HUSK ASH IN CERAMIC MATERIALS USING THE RESPONSE SURFACE METHODOLOGY

Asotah Wisdom*[1], Udochukwu Mark[1], Elakhame Zeberu[2], and Abraham Adeleke[3]

[1]Department of Metallurgical and Materials Engineering, Federal University of Technology, Owerri, Imo State, NIGERIA
[2]Federal Institute of Industrial Research Oshodi, Lagos State, NIGERIA
[3]Department of Materials Science & Engineering, Obafemi Awolowo University, Ile-Ife, NIGERIA

Optimisation of the physical properties of rice husk ash (RHA) in ceramic materials was carried out using Response Surface Methodology. The independent variables, namely the firing temperature and residue content, were statistically combined in a Central Composite Design with the effects on water absorption, linear shrinkage, bulk density, apparent porosity and apparent specific gravity determined. Physical and microstructural analyses were carried out to obtain information on the processes that occurred within the ceramic materials. The results obtained were analysed to determine the optimum physical properties of the ceramic materials within the range investigated. The residue content had a significant influence (at 95% confidence level) on the bulk density, water absorption, apparent porosity and apparent specific gravity but not on the linear shrinkage. The firing temperature had a more significant effect on the linear shrinkage than on the residue content, so that when elevated it contributed to an increase in linear shrinkage. The optimum residue content and firing temperature to enhance physical properties within the range investigated were 5.85% RHA and $1029.64\,°C$, respectively. These optimal conditions are expected to produce a ceramic material with a bulk density, linear shrinkage, apparent porosity, water absorption and apparent specific gravity of 1.64 g/cm^3, 0.29%, 0.29 g/cm^3, 18.26% and 2.11, respectively with a composite desirability of 100%.

Keywords: Ceramics, Rice Husk Ash, Central Composite Design, Linear Shrinkage, Water Absorption

1. Introduction

Global concerns remain with regard to how best to manage the ballooning quantity of waste materials generated on an annual basis. Waste is made up of different materials and could be classified more specifically based on its physical state (solid, liquid, gas), source (agricultural, industrial, mining) or environmental impact (hazardous and non-hazardous waste) [1]. Agricultural (food) waste is common and has been on the rise globally, with an average annual increase of between 5 and 10% [2].

Rice husk ash (RHA) is a residue generated when rice husk is burnt to ashes. Rice husk itself is a form of agricultural waste and a by-product of rice cultivation. Rice is a staple food that is widely cultivated and consumed globally. Therefore, waste generated from its production is abundant. The estimated global production from rice paddies is 600 million tonnes with 21 million tonnes of ash generated per year [3]. Open burning of the husk has a deleterious effect on the environment, polluting our air by the release of harmful gases, smoke and dust particles, which, when inhaled, can cause respiratory diseases [2]. This has led researchers to focus on managing this waste stream to reduce potential environmental concerns.

Rice husk ash has been found to contain a very significant percentage of silica, namely about $85-90\%$ [3, 4]. Given its high silica content, RHA is an excellent potential surrogate to replace quartz in triaxial ceramic bodies [5]. Research has shown that clay-based ceramics can tolerate the incorporation of waste materials in terms of their product formulation. This natural inclination has encouraged researchers to incorporate various industrial and agricultural by-products into ceramic bodies, potentially reducing environmental pollution [5–8].

The introduction of RHA as a substitute for quartz in triaxial ceramic bodies has been found to reduce the thermal expansion and maturing temperature as well as increase the glassy phase while marginally improving their strength. This reduction in the maturing temperature will lead to cost savings in terms of energy consumption, lowering overall production costs [9]. However, the introduction of this type of residue in compositions used to produce ceramic tiles needs to be further analysed. One way

*Correspondence: wisdomasotah@gmail.com

Table 1: Analysed parameters: firing temperature (FT), residue content (RC) – their levels and coded values.

Factor	Coded Levels				
	$-\alpha$	Low	Medium	High	$+\alpha$
	-1.414	-1	0	1	1.414
FT (°C)	1030	1040	1065	1090	1100
RC (%RHA)	5.85	10	20	30	34.12

Figure 1: Fired ceramic samples.

of analysing the effects of replacing rice husk ash in tri-axial ceramic bodies is through the statistical design of experiments, which has many advantages over the one-factor-at-a-time method.

The factorial design of the experiment allows for the simultaneous investigation of the effects (direct and interactive) of two or more independent variables on the dependent variable [10]. Response surface methodology is a powerful statistical tool that allows researchers to develop a second-order polynomial model to determine the optimum condition for an improved response [11].

This study has dual objectives. he first is to create a mathematical model that describes the physical properties (dependent variables) as a function of the firing temperature (FT) and the residue content (RC, in unit %RHA), the independent variables. This modelling is based on the central composite design of experiments and regression analysis, an efficient statistical technique, to determine the regression coefficients that ensure the best fit of the predictive polynomial. Data analysis would involve evaluating the experimental design using various estimates of the regression matrix and model analysis. The second objective was to determine the optimum conditions (FT, RC) that improve its physical properties.

2. Experimental

The following raw materials were used in this study: rice husk collected within Epe, a town in Lagos State; as well as feldspar and kaolin sourced in the vicinity of Ogijo and Shagamu in Ogun State. To evaluate the effect of the FT and RC on the physical properties of the material, Response Surface Methodology combined with Central Composite Design were used. The Central Composite Design method consisted of two factors at two levels, namely 2^2, which yielded 4 cube points with 4 axial (star) points and 5 center points. Minitab 19 Statistical Software (Minitab Inc., USA) was used to design the experiment and analyse the results. Table 1 presents the factors as well as their levels and coded values.

Initially, the kaolin was beneficiated by being soaked in water for 24 hours and then sieved through the mesh of a 150 μm sieve (particles with diameters of less than 150μm down to submicron and nanoparticles passed through). Particles larger than 150μm (predominantly sand, silt and debris) were extracted. The slurry was left to stand and the excess water decanted. The wet clay was air-dried and milled using a ball mill (Model 87002

Limongs – France A50 – 43). Feldspar rock was also milled to particle sizes of less than 150μm. The rice husk ash was dried and sieved to particle sizes of less than 150μm. All the sieving was conducted using a BS 410 sieve to eliminate ions and other debris.

The dry powders were measured in the right proportions according to the experimental design using the coded and uncoded values presented in Table 2 as well as a metro weighing scale with a sensitivity of 0.001 mg. Water was added and the mixture homogenized to make it workable. A quantity of the ceramic composite was put into a metal mould and placed on a press die's mantelpiece. A minimum pressure of 300 kN/m^2 was applied uniaxially upon the sample in the press die. The mould was constantly lubricated to facilitate the easy removal of the composite. The pressed specimens were stored overnight before being dried at 90 ± 100 °C for 48 hrs in an oven (Memmert GmbH, Germany). The dried specimens were fired in a laboratory electric furnace (Thermolyne 46200) at a rate of 5°C/min between 1000 °C and 1100 °C according to the phase change corresponding to the composition of the mixture. The chosen parameters for the firing cycle on a laboratory scale were adapted from the parameters used in industry.

The following physical properties were evaluated: water absorption (WA), bulk density (BD), apparent porosity (AP), apparent specific gravity (AP-SG), and linear shrinkage (LS). The LS was determined from the variation in the linear dimension of the specimen. According to Archimedes' method, WA and BD were determined using water at room temperature as the immersion fluid. The volume of open pores was determined by the AP, while the AP-SG evaluated how impervious the ceramic is to water.

The crystalline phases of the fired samples were analysed by the X-ray diffraction (XRD) technique using a Rigaku MiniFlex Benchtop X-ray Diffractometer. The fracture surfaces of the samples were morphologically characterised by Scanning Electron Microscopy (SEM) using a Phenom ProX SEM and Energy Dispersive X-ray (EDX) analysis determined the elemental composition of the samples. The fired samples are presented in Fig. 1.

3. Results and Discussion

Table 3 describes the elemental composition of the ceramic samples. By analysing the morphology and elemental composition of the various structures, information on the processes that occurred within the ceramic body when subjected to independent variables and on the nature of the minerals was obtained. EDX measurements showed that the ceramic samples were mainly composed of primary metals such as Na, K, Ca, Mg, Fe, Ag and Ti as well as non-metals like P and S – the contents of which vary between samples and even within individual samples depending on the composition of the investigated area.

The high concentrations of Si and Al are related to the raw materials, that is, rice husk ash and kaolin. Silica, an oxide of Si, is commonly found in several mineralogical clay-rich and clay-deficient phases such as kaolin, mica, feldspar and quartz. Alumina, an oxide of Al, is usually associated with some of these mineralogical phases. Potassium (K_2O) and sodium (Na_2O) oxides generally originate from feldspars, hence the presence of P and Na in the EDX data. The low content of Fe is essential to produce white ceramics since it can lead to the development of a reddish colour during sintering [6, 12].

Values of the dependent variables (observed and predicted), namely LS, WA, AP, AP-SG, and BD, from the ceramic samples are listed in Table 4. All values were calculated using the experimental planning matrix produced by Minitab 19 software. The results of the regression analysis, namely the values of the polynomial equation for the dependent variables, are shown in Eqs. 1–5 and the corresponding coefficients of the regression analysis, that is, R-squared (R^2) and adjusted R-squared (R^2(adj.)), are presented in Table 5.

$$BD(g/cm^3) = -28.92 + 0.015\,RC + 0.0572\,FT - 0.000337\,RC^2 - 0.000027\,FT^2 \quad (1)$$

$$WA(\%) = -25.44 + 0.0188\,RC + 0.04789\,FT - 0.000295\,RC^2 - 0.000022\,FT^2 - 0.000006\,RC{\times}FT \quad (2)$$

$$AP_{SG} = -388.1 + 0.233\,RC + 0.730\,FT - 0.003957\,RC^2 - 0.000341\,FT^2 - 0.000062\,RC{\times}FT \quad (3)$$

$$AP(g/cm^3) = -52.50 + 0.0348\,RC + 0.0987\,FT - 0.000596\,RC^2 - 0.000046\,FT^2 - 0.000009\,RC{\times}FT \quad (4)$$

$$LS = -32.7 + 0.0420\,RC + 0.0600\,FT + 0.000104\,RC^2 - 0.000027\,FT^2 - 0.000042\,RC{\times}FT \quad (5)$$

Table 6 shows the regression coefficients obtained when the observed values of LS in Table 4 were fitted to the quadratic model. The statistical significance of each independent variable on this fitting was determined using the P Value, F Statistic on its linear and quadratic terms as well as the interaction between regression coefficients. The smaller the P Value, the more significant the corresponding regression coefficient; P Value < 0.05 indicated that the regression coefficient was statistically significant at 95% confidence interval. As can be seen in Table 6, only the FT exhibited statistical significance over the range investigated. The main regression coefficients (linear and quadratic) for the RC did not show any significance. Therefore, the FT had a more significant effect on changing the LS than the RC.

The LS determines the degree of compaction and densification by analysing the linear variation with regard to the length of the sample after firing, which is essential for

Table 2: Parameters with coded and uncoded values.

Run/Sample	Coded Form of Independent Variables		Uncoded Form of Independent Variables	
	X_1	X_2	X_1	X_2
1	0	0	1065	20
2	0	−1.414	1065	5.8579
3	1	−1	1090	10
4	−1.414	0	1030	20
5	0	0	1065	20
6	1	1	1090	30
7	0	0	1065	20
8	1.414	0	1100	20
9	0	1.414	1065	34.1421
10	0	0	1065	20
11	−1	−1	1040	10
12	0	0	1065	20
13	−1	1	1040	30

X_1 = firing temperature (celsius); X_2 = residue content (%RHA)

Table 3: EDX data of ceramic samples.

Sample	Element (Atomic Concentration %)								
	9	11	4	2	13	3	6	8	7
Si	62.15	57.98	62.44	59.97	58.85	56.15	68.07	58.03	54.70
Al	21.66	27.71	17.12	26.02	24.19	29.44	18.62	28.46	29.07
Fe	3.20	2.78	3.15	2.9	4.51	3.43	1.99	3.32	3.52
K	2.48	1.65	2.72	1.57	2.33	1.75	2.15	1.48	2.19
Na	0.53	0.58	1.43	0.67	0.55	0.54	0.31	0.79	0.39

Table 4: Observed and predicted values of the linear shrinkage (LS), water absorption (WA), bulk density (BD), AP-SG (AP-SG) and apparent porosity (AP).

LS		BD (g/cm^3)		AP		AP-SG		WA	
Observed	Predicted	Observed	Predicted	Observed	Predicted	Observed	Predicted	Observed	Predicted
0.086	0.086	0.086	0.086	0.499	0.499	3.525	3.525	0.283	0.283
0.054	0.087	1.687	1.675	0.371	0.361	2.684	2.605	0.22	0.216
0.135	0.962	1.683	1.701	0.384	1.403	2.732	2.868	0.228	0.236
0.026	0.023	1.72	1.726	0.421	0.436	2.968	3.059	0.245	0.253
0.086	0.086	0.086	0.086	0.499	0.499	3.525	3.525	0.283	0.283
0.114	0.103	1.722	1.731	0.421	0.425	2.972	3.018	0.244	0.245
0.086	0.086	0.086	0.086	0.499	0.499	3.525	3.525	0.283	0.283
0.051	0.081	1.752	1.735	0.462	0.446	3.259	3.137	0.264	0.257
0.133	0.127	1.717	1.718	0.389	0.399	2.814	2.862	0.227	0.232
0.086	0.086	0.086	0.086	0.499	0.499	3.525	3.525	0.283	0.283
0.05	0.034	1.694	1.696	0.395	0.391	2.798	2.782	0.233	0.231
0.086	0.086	0.086	0.086	0.499	0.499	3.525	3.525	0.283	0.283
0.071	0.083	1.733	1.726	0.441	0.423	3.1	2.995	0.255	0.246

Table 5: Relevant statistics for the analysis of variance of the mathematical models that describe the variables BD, AP, AP-SG, WA and LS.

Variable	Model	F Statistic	P Value	R^2	R^2(adj.)
BD	Quadratic	15.78	0.001	0.92	0.86
AP	Quadratic	29.38	0	0.95	0.92
AP-SG	Quadratic	29.58	0	0.95	0.92
WA	Quadratic	30.06	0	0.96	0.92
LS	Quadratic	2.95	0.096	0.68	0.45

Table 6: Statistics for the analysis of the variance of the model that describes linear shrinkage (LS).

Model Term	Regression Coeff.	P Value	F Statistic
Intercept	-32.7	-	-
RC	0.042	0.144	2.7
FT	0.06	0.047	5.78
RC^2	0.000104	0.292	1.3
FT^2	-0.000027	0.102	3.54
RC$\times$FT	-0.000042	0.411	0.76

controlling the dimensions of the finished ceramic product [6]. The model yielded a positive value (0.06) for the regression coefficient of the FT (Eq. 5), suggesting that the FT is directly dependent on the LS. It is expected that as the temperature rises, the degree of LS increases. As the temperature rises during firing, a more significant amount of the liquid phase is produced and its viscosity decreases. This facilitates the elimination of pores, thereby increasing the extent of LS. The adequacy of the model was determined by the correlation coefficient R, which was calculated as 0.68, moreover, the high P Value and low coefficient of determination are indicative of the model's considerable degree of variability (Table 5). The data points in the normal percentage distribution curves shown in Fig. 2 lie close to the line indicating no significant deviation from normality nor any need for response transformation. The residual versus fitted plot should resemble a scatter plot as shown in Fig. 3. If the plots do not present a random scattering of data as represented in Fig. 2, then any trends will indicate flaws in the assumptions [6, 11].

Regression coefficients obtained when the observed values of BD, WA, AP and AP-SG were fitted in the quadratic model are shown in Tables 7–10, respectively. The main independent variable, namely the FT, did not exhibit any significance over the range investigated. Among the interacting regression coefficients shown in Tables 7–10, interactions between the RC and FT were not found to be statistically significant.

The WA capacity is directly related to the type of microstructure that developed while the samples were sin-
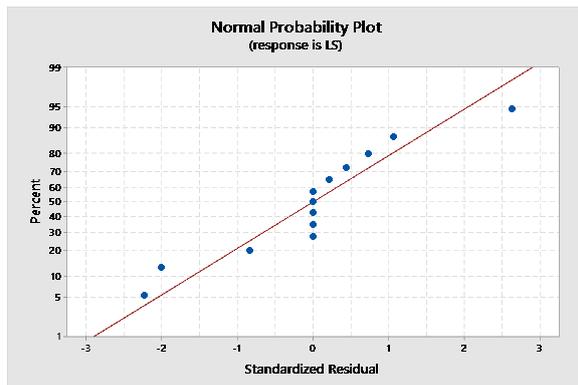
Figure 2: Normal probability plot of the residual plot for linear shrinkage (LS).
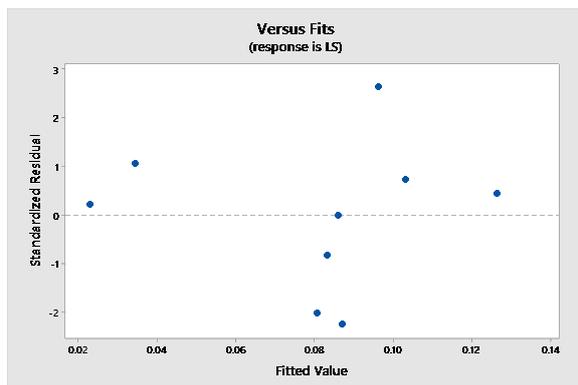

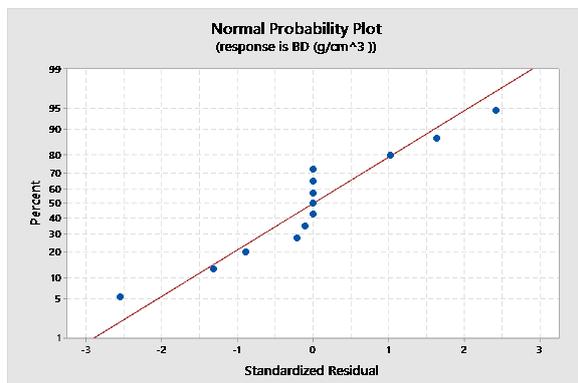*Figure 3:* Residual plot against the fitted plot for linear shrinkage (LS).

Figure 4: Normal probability plot of the standardized residual of the bulk density (BD).

Table 7: Statistics for analysis of variance of the model that describes the bulk density (BD).

Model Term	Regression Coeff.	P Value	F Statistic
Intercept	-28.92	-	-
RC	0.015	0.008	13.14
FT	0.0572	0.506	0.49
RC^2	-0.000337	0	57.44
FT^2	-0.000027	0.007	14.15
RC$\times$FT	0	1	0

Table 8: Statistics for analysis of variance of the model that describes water absorption (WA).

Model Term	Regression Coeff.	P Value	F Statistic
Intercept	-25.44	-	-
RC	0.0188	0.043	6.08
FT	0.04789	0.593	0.31
RC^2	-0.000295	0	128.25
FT^2	-0.000022	0.001	28.88
RC$\times$FT	-0.000006	0.676	0.19

Table 9: Statistics for analysis of variance of the model that describes apparent specific gravity (AP-SG).

Model Term	Regression Coeff.	P Value	F Statistic
Intercept	-388.1	-	-
RC	0.233	0.031	7.23
FT	0.73	0.447	0.65
RC^2	-0.003957	0	119.58
FT^2	-0.000341	0.001	34.79
RC$\times$FT	0.000062	0.755	0.11

Table 10: Statistics for analysis of variance of the model that describes apparent porosity (AP).

Model Term	Regression Coeff.	P Value	F Statistic
Intercept	-52.5	-	-
RC	0.0348	0.03	7.33
FT	0.0987	0.522	0.45
RC^2	-0.000596	0	123.29
FT^2	-0.000046	0.001	28.91
RC$\times$FT	-0.000009	0.76	0.1

tering and its level of porosity. This is regarded as a simple way to predict the technological properties of the final products [6, 13]. Within the range investigated, the RC was shown to be more dependent on the WA, BD, AP and AP-SG, which is in good agreement with the model prediction.

The adequacy of this prediction is confirmed by the coefficient of determination, R^2, values of BD, AP, AP-SG and WA which were calculated to be 0.92, 0.95, 0.95 and 0.96, respectively (Table 5). The high values of R^2 given as 0.86, 0.92, 0.92 and 0.92 (Table 5) indicate that the adjusted models do not present a considerable degree of variability. This is also evident on the normal percent-

age distribution curve and the residuals versus fits plot (Figs. 4 and 5, respectively), which show that the data set is normally distributed and falls within $(-2, 2)$ for BD. Furthermore, similar plots are produced for WA, AP and AP-SG with a statistical significance of 95% and less than 5% as outliers observed.

Fig. 6 shows the XRD patterns of the ceramic samples with RCs of 5.85% and 34.14%, that is, the lowest and highest RCs studied in the present work. According to the XRD patterns, all the ceramic samples consisted of similar minerals, namely kaolinite [$Al_2Si_2O_5(OH)_4$], montmorillonite [$NaMgAlSiO_2(OH)H_2O$], suessite [Fe_3Si], and illite [$KAl_2Si_3AlO_10(OH)_2$]. With RCs of 34.14%,
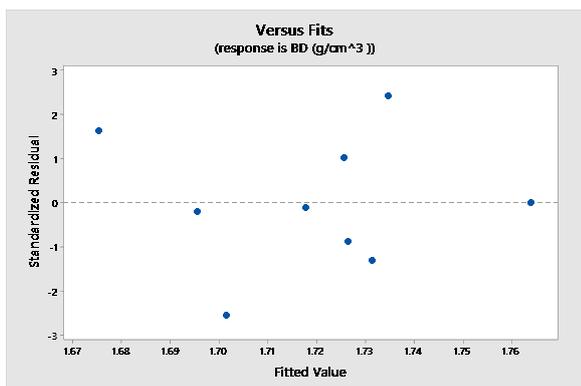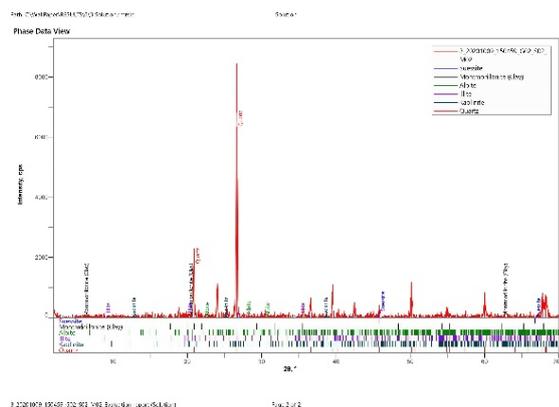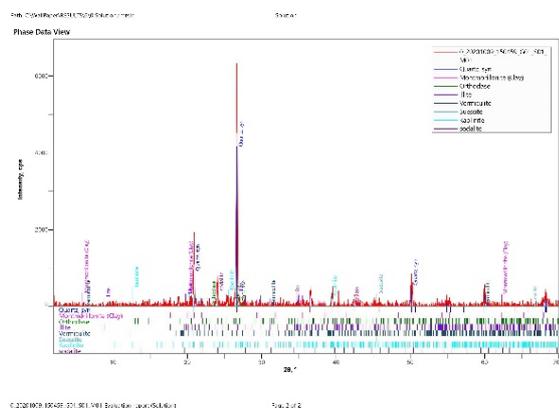
Figure 5: Plot of the standardized residual against the fitted values of the bulk density (BD).

(a) 5.86% RHA

(b) 34.14% RHA

Figure 6: XRD patterns of samples against their RCs (%RHA).

orthoclase and synthesised quartz were present. Quartz exhibited the highest peak, which confirms the high concentration of Si according to the EDX data. Little or no difference was detected between the intensities of the peaks. All ceramic samples contained clay minerals; quartz, kaolinite, illite and albite are the mineral phases of the raw materials used.

The micrograph (Fig. 7) shows that the ceramic matrix of samples sintered at higher temperatures (1090 °C
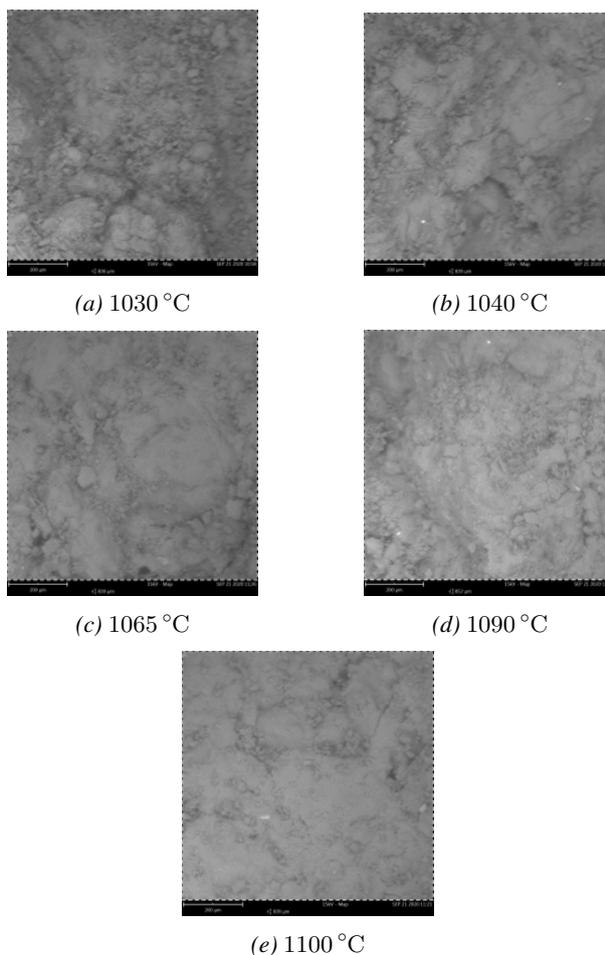

(a) 1030 °C

(b) 1040 °C

(c) 1065 °C

(d) 1090 °C

(e) 1100 °C

Figure 7: SEM micrograph of fracture surfaces of ceramic samples against RC.

and 1100 °C) was more finely dispersed and densely packed. A reduction in porosity was observed compared to samples sintered at lower temperatures (1030 °C, 1040 °C and 1065 °C) which were more porous and irregular as at higher sintering temperatures. As observed, increase in FT led to an increase in vitreous phase, facilitating the elimination of pores and an increase in densification. This hypothesis is in good agreement with other research [6, 12, 13].

3.1 Response optimisation

The optimised responses with regard to the physical properties of ceramics in which rice husk ash is used as a silica precursor and their criteria are presented in Table 11, moreover, the desired quality is shown in Fig. 8. From the optimisation results and plot presented in Fig. 8, the optimum RC and FT to achieve the desirable physical properties are 5.85% and 1029.64 °C, respectively. These optimal conditions are expected to produce a ceramic product with a BD of 1.64 g/cm^3, LS of 0.29, AP of 0.29 g/cm^3, WA of 18.26%, and AP-SG of 2.11.

The optimal combination of the factors shown in Fig. 8 effectively maximises the LS as well as minimises the
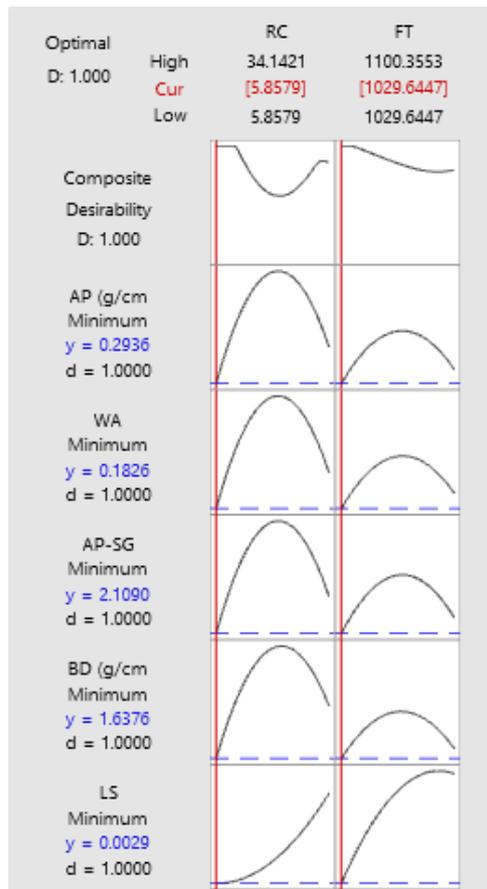
Figure 8: Optimisation plot of the variables.

possible to obtain significant mathematical models which correlate the factors FT and RC with the dependent variables LS, WA, AP, AP-SG, and BD. The FT had a statistically significant effect on the LS so that raising the temperature enhanced the degree of shrinkage. However, the RC had a more significant effect on the BD, AP, AP-SG, and WA. It can be concluded that the optimum physical properties within the range investigated are a BD of 1.64 g/cm^3, LS of 0.29, AP of 0.29 g/cm^3, WA of 18.26%, and AP-SG of 2.11 with a RC of 5.85% and a FT of $1029.64\,°C$. The composite desirability to achieve the optimal settings is 100% and yielded favourable results for all responses when the objective functions were considered simultaneously.

REFERENCES

[1] Amasuomo, E.; Baird, J.: The concept of waste and waste management, *J. Manage. Sust.,* 2016, **6**(4), 88–96 DOI: 10.5539/jms.v6n4p88

[2] Wang, B.; Dong, F.; Chen, M.; Zhu, J.; Tan, J.; Fu, X.; Wang, Y.; Chen, S.: Advances in recycling and utilisation of agricultural wastes in China: Based on environmental risk, crucial pathways, influencing factors, policy mechanism. *Procedia Env. Sci.,* 2016, **31**, 12–17 DOI: 10.1016/j.proenv.2016.02.002

[3] Jamo, U.; Maharaz, M. N.; Pahat, B.: Influence of addition of rice husk ash on porcelain composition. *Sci. World J.* 2015, **10**(1), 7–16 https://www.ajol.info

[4] De Silva, G. H. M. J. S.; Surangi, M. L. C.: Effect of waste rice husk ash on structural, thermal and run-off properties of clay roof tiles. *Constr. Build. Mater.,* 2017, **154**, 251–257 DOI: 10.1016/j.conbuildmat.2017.07.169

[5] Correia, S. L.; Dienstmann, G.; Folgueras, M. V.; Segadaes, A. M.: Effect of quartz sand replacement by agate rejects in triaxial porcelain. *J. Hazard. Mater.,* 2009, **163**(1), 315–322 DOI: 10.1016/j.jhazmat.2008.06.094

[6] Silva, K. R.; Campos, L. F. A.; de Lima Santana, L. N.: Use of experimental design to evaluate the effect of the incorporation of quartzite residues in ceramic mass for porcelain tile production. *Mater. Res.,* 2018, **22**(1), 1–11 DOI: 10.1590/1980-5373-MR-2018-0388

[7] Bragança, S. R.; Vicenzi, J.; Guerino, K.; Bergmann, C. P.: Recycling of iron foundry sand and glass waste as raw material for production of whiteware. *Waste Manage. Res.,* 2006, **24**(1), 60–66 DOI: 10.1177/0734242X06061155

[8] Ogunro, A. S.; Apeh, F. I.; Nwannenna, O. C.; Ibhadode, O.: Recycling of waste glass as aggregate for clay used in ceramic tile production. *Am. J. Eng. Res.,* 2018, **7**(8), 272–278 http://www.ajer.org

[9] Vernon, E.: Substitution of rice husk ash for quartz in ceramic wall tiles (PhD Thesis), Department of Industrial Design 2015

BD, WA, AP-SG, and AP. The composite desirability of 100% showed how the settings optimise all five quality responses when they are considered as objective response functions simultaneously [11].

4. Conclusions

The physical properties of the ceramic samples using the response surface methodology were optimised. The modelling was based on central composite design and it was

Table 11: Criteria and results of the optimisation of the process conditions.

Response	Goal	Response	Desirability
Linear Shrinkage (%)	Minimum	0.29	100%
Bulk Density (g/cm^3)	Minimum	1.64	100%
Apparent Porosity (g/cm^3)	Minimum	0.29	100%
Apparent Specific Gravity	Minimum	2.11	100%
Water Absorption (%)	Minimum	18.26	100%
Composite desirability – 100%			

[10] Halim, R.; Webley, P. A.: Nile red staining for oil determination in microalgal cells: A new insight through statistical modelling. *Int. J. Chem. Eng.,* 2015, **2015**(695061) DOI: 10.1155/2015/695061

[11] Ogunbiyi, M. O.: Optimisation of parboiling process using response surface methodology (RSM) to improve the physical properties of parboiled milled rice. *Int. J. Eng. Res. Technol.,* 2018, **V7**(07), 312–318 DOI: 10.17577/ijertv7is070117

[12] Oancea, A. V.; Bodi, G.; Nica, V.; Ursu, L. E.; Drobota, M.; Cotofana, C.; Vasiliu, A. L.; Simionescu, B. C.; Olaru, M.: Multi-analytical characterization of cucuteni pottery. *J. Eur. Ceramic Soc.,* 2017, **37**(15), 5079–5098. DOI: 10.1016/j.jeurceramsoc.2017.07.018

[13] Torres, P.; Manjate, R. S.; Quaresma, S.; Fernandes, H. R.; Ferreira, J. M. F.: Development of ceramic floor tile compositions based on quartzite and granite sludges. *J. Eur. Ceramic Soc.,* 2007, **27**(16), 4649–4655 DOI: 10.1016/j.jeurceramsoc.2007.02.217